J. Fluid Mech. (1984), *vol.* 142, *pp.* 233–249
Printed in Great Britain

Internal waves in a horizontally inhomogeneous flow

By A. Ya. BASOVICH AND L. Sh. TSIMRING
Institute of Applied Physics, Academy of Sciences of the USSR, Gorky, USSR

(Received 28 October 1982 and in revised form 28 November 1983)

The effect of horizontally inhomogeneous flows on internal wave propagation in a stratified ocean with a constant Brunt–Väisälä frequency is analysed. Dispersion characteristics of internal waves in a moving fluid and kinematics of wave packets in smoothly inhomogeneous flows are considered using wave-normal surfaces. It is shown that internal-wave blocking and short-wave transformation may occur in longitudinally inhomogeneous flows. For parallel flows internal-wave trapping is possible in the vicinity of the limiting layer where the wave frequency in the locally comoving frame of reference coincides with the Brunt–Väisälä frequency. Internal-wave trapping also takes place in jet-type flows in the vicinity of the flow-velocity maximum. WKB solutions of the equation describing internal-wave propagation in a parallel horizontally inhomogeneous flow in the linear approximation are obtained. Singular points of this equation and the related effect of internal-wave amplification (overreflection) under the action of the flow are investigated. The spectrum and the growth rate of internal-wave localized modes in a jet-type flow are obtained.

1. Introduction

The presence of large-scale oceanic quasi-stationary motions, in particular frontal currents and rings, changes the character of internal-wave propagation essentially, especially so when flow and internal-wave velocities are much the same. The effect of inhomogeneous flows on internal waves has been experimentally investigated in the ocean (see e.g. Frankignoul 1974; Ruddick & Joyce 1979) and in the laboratory (Thorpe 1981). The theoretical studies have principally dealt with the analysis of internal-wave propagation in vertically sheared flows (e.g. Booker & Bretherton 1967; Fritts 1978). The distinctive characteristics of this propagation are internal-wave reflection at the level where the wave frequency in the locally comoving frame of reference coincides with the Brunt–Väisälä frequency, and wave trapping in the vicinity of the critical layer where the above frequency vanishes.

Available experimental data (see e.g. MODE Group 1978) are indicative of considerable horizontal inhomogeneity of the current field in the ocean. Therefore analysis of internal-wave propagation in flows with horizontal variation of velocity is of interest. A similar problem has been considered by Olbers (1981), who analysed the internal-wave trajectories in parallel flows. Propagation of Rossby–gravity waves in a rotating stratified flow has been investigated by Ahmed & Eltayeb (1980). The present paper deals with the effect of horizontally inhomogeneous flows on short-period internal waves within the framework of a simple model with the Brunt–Väisälä frequency and flow velocity independent of depth.

Here we consider the two most typical cases: flows inhomogeneous along the

direction of velocity ($\nabla|\boldsymbol{U}| \parallel \boldsymbol{U}$) and parallel flows ($\nabla|\boldsymbol{U}| \perp \boldsymbol{U}$).† The scale of flow inhomogeneity is assumed to be much larger than the internal-wave wavelength, and the WKB method is used. First, internal-wave kinematics in smoothly inhomogeneous flows is investigated for both cases. The consideration is based on a detailed analysis of dispersion characteristics of waves in a moving fluid using wave-normal surfaces (WNS). Then the case of parallel flows is studied in more detail. In this case features, in particular of resonant character, may occur. To analyse them, equations describing an internal-wave field in the presence of a horizontally inhomogeneous parallel flow are used. Internal waves are shown to intensify or attenuate owing to the interaction with the flow. They may also be trapped in the vicinity of the layer where the Doppler-shifted frequency of the wave coincides with the Brunt–Väisälä frequency. Localized waves may occur in flows with a jet velocity profile. Under certain conditions these waves may grow exponentially in space or time.

2. Internal-wave kinematics in a horizontally inhomogeneous flow

2.1. *Wave-normal surfaces*

A dispersion equation for internal waves in a uniformly stratified fluid moving at a speed $\boldsymbol{U} = U\boldsymbol{x}_0$ has the form (see Phillips 1977)

$$\Omega^2 \equiv (\omega - \boldsymbol{k}\cdot\boldsymbol{U})^2 = \frac{N^2(k_x^2+k_y^2)}{k_x^2+k_y^2+k_z^2}, \tag{2.1}$$

or in the explicit form

$$\omega = k_x U \pm N\left(\frac{k_x^2+k_y^2}{k_x^2+k_y^2+k_z^2}\right)^{\frac{1}{2}}, \tag{2.2}$$

where ω and $\boldsymbol{k}(k_x, k_y, k_z)$ are the frequency and the wavevector of the internal wave (z is the vertical and x and y are the horizontal coordinates), Ω is the Doppler-shifted frequency of the wave, N is the Brunt–Väisälä frequency. WNS (ω = const) in conformity with (2.1) are the surfaces in a three-dimensional $\boldsymbol{k}$-space. To investigate the cases of longitudinally inhomogeneous and parallel flows, cross-sections of these surfaces by the planes $k_y = k_{y0}$ and $k_z = k_{z0}$ respectively are required.

Plots of WNS ($\omega > 0$) in the plane (k_x, k_z) for different U are given in figure 1. The arrows show the direction of the wave group velocity. For simplicity the plots are given for $k_{y0} = 0$.‡ Figure 1 (*a*) corresponds to a stagnant fluid. The angle between the lines is defined by the frequency ω. When the fluid moves, anisotropy occurs and the form of the WNS changes (figure 1 (*b*)). The lines depicted in figure 1 (*a*) bend, lock at the point $k_x = (\omega - N)/U$ forming a 'loop' at $k_x < 0$, and tend asymptotically to the line $k_x = \omega/U$ at $k_x > 0$. To the right of this line branch II appears which corresponds to the negative sign in (2.2), i.e. $\Omega < 0$.

Branch II corresponds to waves with negative energy density (Whitham 1974; Acheson 1976). These are slow waves: their phase velocity $c = \omega/k_x$ is smaller than the flow velocity. Physically the negative energy density means that the total energy density of a fluid with excited slow waves is smaller than the energy density of the flow in the absence of perturbations. The fact that the energy density of the waves with $\Omega < 0$ is negative follows from the average variational principle (Whitham

† The first type of flow does not satisfy the continuity equation, and there is always a horizontal or a vertical component of flow velocity perpendicular to $\boldsymbol{U}$. However, if it is small, the idealization ($\boldsymbol{U} = U(x)\boldsymbol{x}_0$) is reasonable, as is evidenced by the consideration given below.

‡ In a more general case $k_{y0} \neq 0$ the behaviour of the curves is different from that shown in figure 1 only in the vicinity of the origin; in this case the WNS cross the axis k_z in two points (at $k_z \neq 0$).

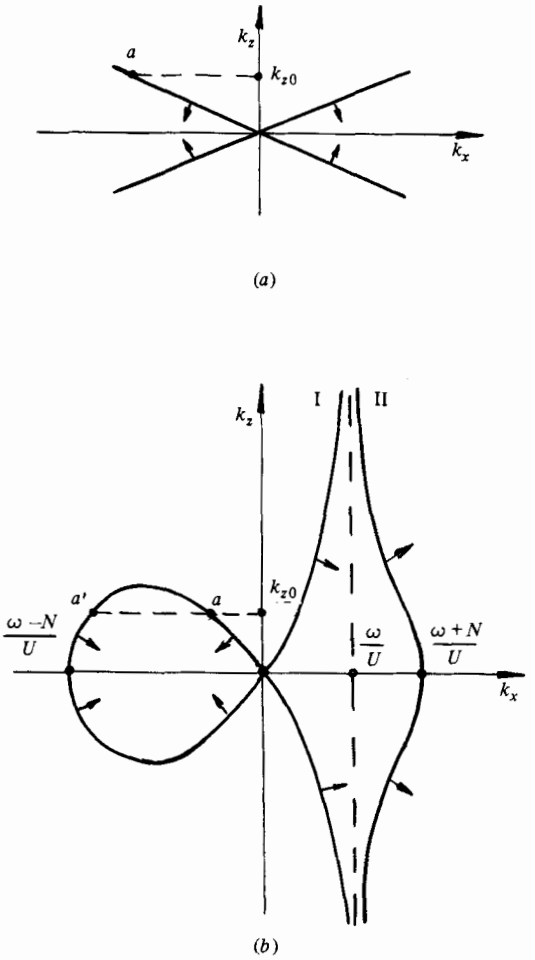

FIGURE 1. Plots of WNS in a moving fluid on the (k_x, k_z)-plane at $k_y = 0$: (*a*) $U = 0$; (*b*) $U > 0$.

1974). According to this principle in the linear approximation the energy density of the wave $W = \Omega\, \partial\mathscr{L}/\partial\omega$, where $\mathscr{L}$ is the mean Lagrangian density, $\partial\mathscr{L}/\partial\omega$ is the wave-action density invariant with respect to the reference system. This invariant is a positive value, which is readily proved when the wave is considered in the reference system with a motionless fluid. Therefore the energy density of the wave in the laboratory system is negative at $\Omega < 0$. As $U \to 0$ branch II goes to infinity. A segment of branch I which has a positive x-component of the group velocity corresponds to backward waves ($\boldsymbol{k} \cdot \boldsymbol{V}_{\mathbf{g}} < 0$).

Figure 2 gives plots of WNS in the (k_x, k_y) plane at $k_z = k_{z0}$. These curves are similar to WNS of the waves on the surface of a moving fluid studied by Basovich & Talanov (1977). At $U = 0$ (figure 2 (*a*)) the WNS are isotropic and have the form of a circumference. Two more branches appear in the moving fluid: I″ – backward waves, and II – slow waves with a negative energy density (figure 2 (*b*)). As the flow velocity grows, branches I′ and I″ converge, encounter at

$$U_0 = \frac{(N^{\frac{2}{3}} - \omega^{\frac{2}{3}})^{\frac{3}{2}}}{k_{z0}}, \tag{2.3}$$

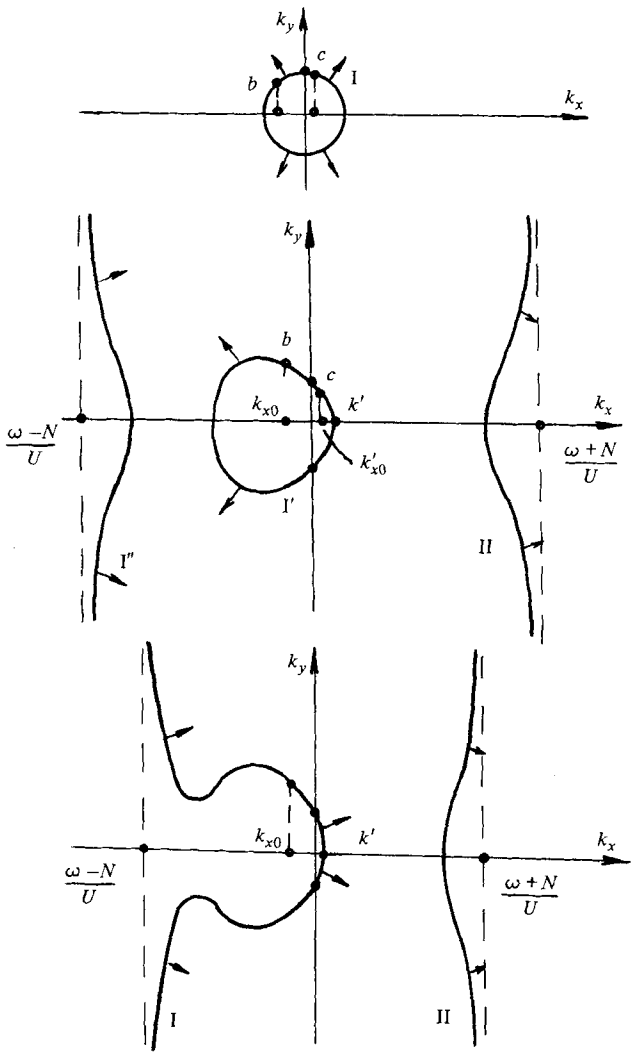

FIGURE 2. Plots of WNS in a moving fluid on the (k_x, k_y)-plane at $k_z = k_{z0}$: (*a*) $U = 0$; (*b*) $0 < U < U_0$; (*c*) $U > U_0$.

and transform to a single branch at $U > U_0$ (figure 2*c*). Branches I and II have vertical asymptotes at the points

$$k_{x\mathrm{I}} = \frac{\omega - N}{U}, \quad k_{x\mathrm{II}} = \frac{\omega + N}{U}. \tag{2.4}$$

The plotted WNS enable one to describe propagation of internal-wave packets in smoothly inhomogeneous flows of a stratified fluid.

2.2. *The longitudinally inhomogeneous flow*

The wave-vector component transverse to $\boldsymbol{U}$ is not changed by a longitudinally inhomogeneous flow $\boldsymbol{U} = U(x)\,\boldsymbol{x}_0$, and the wave frequency does not vary in a stationary flow. Consider a wave packet which moves from the region of the stagnant fluid in the direction opposite to the flow with a negative velocity gradient $\mathrm{d}U/\mathrm{d}x < 0$

and which has vector $\boldsymbol{k}(k_{x0}, 0, k_{z0})$ in this region.† This corresponds to point a in figure 1 (a). Moving against the flow to the region of U increase, the packet slows down, and at $U = U_0$ (2.3) stops ($V_{gx} = 0$, the top of the 'loop' in figure 1 (b) where points a and a' coincide). This effect known for surface gravity waves is called 'blocking' (Gargett & Hughes 1972; Phillips 1973; Smith 1975; Basovich & Talanov 1977). In the blocking point the packet reflects as a group of backward waves (point a' in figure 1 (b)). In the reflected packet, wave crests move against the flow, while the envelope moves along the flow. At the same time k_x grows unlimitedly as U decreases.

Internal-wave-packet blocking may also occur in flows with a positive velocity gradient ($\mathrm{d}U/\mathrm{d}x > 0$), provided that the backward waves have been excited. If the flow velocity is a non-monotonic function of the x-coordinate, packet trapping is possible in the region of its minimum velocity bounded by two blocking points.‡

2.3. *The parallel flow*

The parallel flow $\boldsymbol{U} = U(y)\boldsymbol{x}_0$ does not change components k_x and k_z of the internal-wave vector and its frequency. To analyse the motion of wave packets in such a flow, let us use the WNS given in figure 2. (It should be noted that these WNS can also be used for the previous case. However, when the waves are investigated in a longitudinally inhomogeneous flow (2.2) figure 1 seems to be more demonstrative.)

Consider a wave packet moving at an angle to the direction of the flow with $V_{gx} < 0$, $k_{x0} < 0$ and $k_y > 0$ (point b, figure 2 (a)). Assume that the flow velocity increases in the direction of wave propagation $\mathrm{d}U/\mathrm{d}y > 0$. It is easy to see that the component of the group velocity V_{gy} does not change the sign while V_{gx} changes its sign at a certain point. At $U = (\omega - N)/k_{x0}$, k_{x1} and k_{x0} coincide and a specific layer appears ($V_{gy} \to 0$, $k_y \to \infty$). Since the waves cannot propagate beyond this layer, let us call it a limiting layer. As shown below, the limiting layer in a horizontally inhomogeneous flow and the critical layer in a vertically inhomogeneous one are very much alike. The wave amplitude in the vicinity of such layers tends to infinity, thus dissipation, nonlinearity or other saturating factors should be taken into account.

If the packet moves with $V_{gx} > 0$, $k'_{x0} > 0$ and $k_y > 0$ (point c in figure 2) in a flow with $\mathrm{d}U/\mathrm{d}y > 0$, k'_{x0} and k' coincide at a certain velocity U and the wave reflects. At the same time k_y and V_{gy} change the sign. Using WNS one can also trace packet localization in a flow with jet-type profile. This problem is discussed in detail in §5.

The consideration performed applies not only to internal-wave packets propagating along the z-axis but also to waves with a mode structure (in a stratified fluid layer between the rigid boundaries). For this purpose it suffices to present the mode as a superimposition of two waves with opposite signs and equal values of k_z.

† The case $k_y = 0$ is considered. Similar effects also occur at $k_y \neq 0$. However, the approximation assumed for a longitudinally inhomogeneous flow is valid only at small k_y. At large k_y a flow $\boldsymbol{U}(x, y)$ should be considered and the variation of k_y taken into account.

‡ Using WNS one can similarly trace internal-wave propagation in a flow with a vertical velocity shear $\boldsymbol{U} = U(z)\boldsymbol{x}_0$. For this purpose $k_x = k_{x0}$ must be fixed in figure 1. It is easy to see that the packet moving against the flow reflects at point z_*, which is defined by the relation $N - k_{x0}U(z_*) = \omega$. Unlike in blocking, reflection in this case is accompanied by transition of the representative point to the symmetrical branch of WNS. As the packet moving along the flow approaches the layer where $U = c \equiv \omega/k_{x0}$, the vertical component of the wavenumber $k_z(z)$ increases and the vertical component of the group velocity decreases. This is known as a 'critical' layer (Booker & Bretherton 1967).

3. The equation for an internal wave in a parallel flow and its WKB solutions

Kinematic consideration of internal waves should be supplemented by a transfer equation. This equation for smoothly inhomogeneous flows follows from conservation of the density of the wave action (Whitham 1974). Behaviour of the waves on caustics, for example at blocking points, may be determined in a manner similar to that used by Basovich & Talanov (1977). Therefore the case of a longitudinally inhomogeneous flow is not analysed in detail in this paper.

Below we concentrate our attention on internal waves in parallel flows. Here a number of features associated with the presence of limiting and synchronism points makes analysis of the wave equation necessary. The latter is obtained from a linearized set of equations for an incompressible nonviscid stratified fluid, which in the Boussinesq approximation has the form

$$\left.\begin{aligned} &\frac{\mathrm{D}u}{\mathrm{D}t}+U'v+\frac{1}{\rho}\tilde{p}_x=0, \quad \frac{\mathrm{D}v}{\mathrm{D}t}+\frac{1}{\rho}\tilde{p}_y=0,\\ &\frac{\mathrm{D}w}{\mathrm{D}t}+\sigma+\frac{1}{\rho}\tilde{p}_z=0, \quad \frac{\mathrm{D}\sigma}{\mathrm{D}t}-N^2w=0,\\ &u_x+v_y+w_z=0. \end{aligned}\right\} \tag{3.1}$$

Here u, v and w are respectively the x-, y- and z-components of the velocity perturbation, $\tilde{p}$ is the pressure perturbation, ρ is the mean density, $\sigma=-g\tilde{\rho}/\rho$, $\tilde{\rho}$ is the density perturbation, $N^2=-g\rho_z/\rho$, $\mathrm{D}/\mathrm{D}t=\partial/\partial t+U(y)\,\partial/\partial x$, the indices denote differentiation with respect to the corresponding coordinate, and $U'=\mathrm{d}U/\mathrm{d}y$. The system (3.1) reduces to

$$\left(\frac{\mathrm{D}}{\mathrm{D}t}\right)^3\Delta\tilde{p}-2U'\left[\left(\frac{\mathrm{D}}{\mathrm{D}t}\right)^2+N^2\right]\tilde{p}_{xy}+N^2\frac{\mathrm{D}}{\mathrm{D}t}(\tilde{p}_{xx}+\tilde{p}_{yy})=0, \tag{3.2}$$

where $\Delta=\partial^2/\partial x^2+\partial/\partial y^2+\partial/\partial z^2$. For the amplitude of a sinusoidal wave

$$\tilde{p}=p(y)\exp\left[\mathrm{i}(k_x x+k_z z-\omega t)\right], \quad \frac{\omega}{k_x}=c,$$

an ordinary differential equation is available (cf. Barcilon & Drazin 1972):

$$p''-\frac{2U'}{U-c}p'+\left[k_z^2\frac{U-c}{\left(\frac{N}{k_x}\right)^2-(U-c)^2}-k_x^2\right]p=0. \tag{3.3}$$

Substitution of the variable $p=(U-c)\,\xi$ in (3.3) yields

$$\xi''+K^2(y)\,\xi=0, \tag{3.4}$$

where

$$\left.\begin{aligned} K^2(y)&=n^2+\frac{\Omega''}{\Omega}-2\left(\frac{\Omega'}{\Omega}\right)^2,\\ n^2&=k_z^2\frac{\Omega^2}{N^2-\Omega^2}-k_x^2. \end{aligned}\right\} \tag{3.5}$$

Equation (3.4) is similar to the Schrödinger equation for a particle in a potential hump $-K^2(y)$. For a smooth hump, that is when the scale of inhomogeneity is large

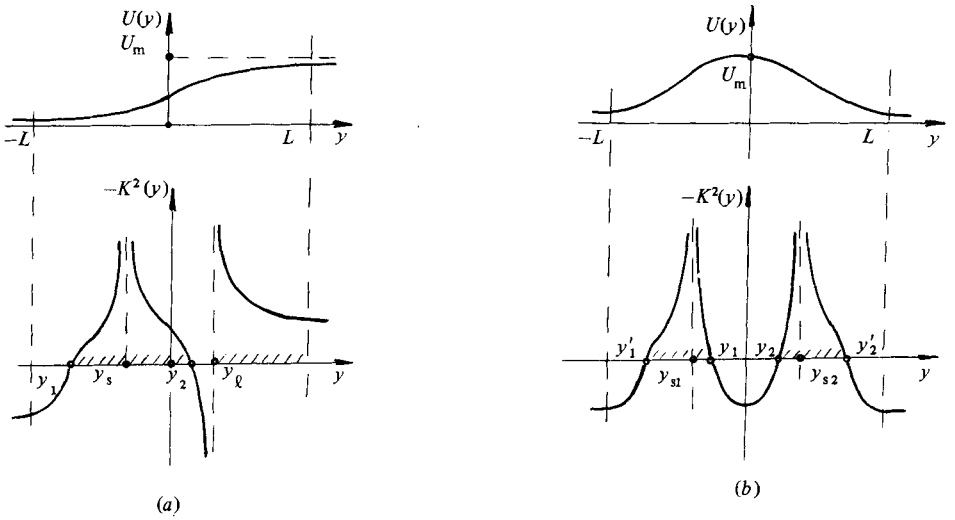

FIGURE 3. 'Potential hump'-$K^2(y)$ of internal waves in a shear flow (a) and in a flow with a jet-type velocity profile (b).

compared to the wavelength, (3.4) has two linearly independent WKB solutions of the form

$$\xi_{1,2} = [K^2(y)]^{-\frac{1}{4}} \exp\left\{\pm i \int [K^2(y)]^{\frac{1}{2}} dy\right\} \tag{3.6}$$

To illustrate the solutions (3.6), figure 3(a) shows a 'potential hump' (3.5) in a shear flow

$$U(y) = \frac{U_m}{2}\left[1 + \tanh\left(\frac{y}{L}\right)\right], \tag{3.7}$$

assuming that $k_x > 0$, $U_m > (\omega + N)/k_x$ and $\omega < N$. Singularities of the potential hump reveal at points where $U(y_s) = \omega/k_x$ and $U(y_\ell) = (\omega + N)/k_x$. Let us refer to points y_s as points of synchronism, since here the flow velocity coincides with the phase speed of the wave, and to y_ℓ as limiting points. The WKB approximation is irrelevant in the vicinity of these points as well as near the turning points where $K^2(y) = 0$; the role of these points is elucidated in §4. As seen from figure 3(a), the waves incident to the region of the shear flow reflect at the turning point y_1 behind which there is a non-transparency region. The wave partially transits into the region of propagation $y > y_2$ bounded by the limiting layer y_ℓ. At $U > U(y_\ell)$, i.e. at $y > y_\ell$, the waves with the given ω and k_x cannot exist, since the modulus of the wave frequency in the locally comoving frame of reference $\Omega = \omega - k_x U$ exceeds that of the Brunt–Väisälä frequency: $|\Omega| > N$. In the non-transparency region (y_1, y_2) there is a point of synchronism $y = y_s$ in which singularity of the coefficients in (3.4) occurs. Location of the point of synchronism in the non-transparency region does not reveal it kinematically. However, as shown in §§4 and 5, it essentially influences wave propagation.

4. The wave-reflection coefficient

Owing to the singularities of the potential hump mentioned in §3, the coefficient of internal-wave reflection at a shear flow is different from unity. To determine the coefficient one should construct an asymptotic solution of (3.4) for the entire region

y, matching WKB solutions of (2.6) at the turning points y_1 and y_2 and at the singular points y_s and y_ℓ with allowance made for the boundary condition at $y \to \infty$. Solution matching at turning points is accomplished in the conventional way (see e.g. Bender & Orszag 1978) and is not considered here. To define the rules of matching at points y_s and y_ℓ one should use standard equations representing the basic features of the solution of (3.4) in the vicinity of these points. The solution in the vicinity of the point y_ℓ is sought for under the condition

$$\left| k_y^2 \frac{\Omega^2}{N^2 - \Omega^2} \right| \gg \left| k_x^2 + \frac{2\Omega'^2}{\Omega^2} - \frac{\Omega''}{\omega} \right|.$$

Making an expansion

$$U = U'(y - y_\ell) + O(y - y_\ell)^2,$$

one obtains

$$\xi'' - \frac{A}{y - y_\ell}\xi = 0, \quad A = \frac{Nk_z^2}{2k_x U'(y_\ell)}. \tag{4.1}$$

Equation (4.1) emerges in various problems, in particular in the theory of hydrodynamic stability. Its solution is

$$\xi = \xi_0 (y - y_\ell)^{\frac{1}{2}} Z_1\{2\mathrm{i}[A(y - y_\ell)]^{\frac{1}{2}}\}, \tag{4.2}$$

where Z_1 is an arbitrary Bessel function of the first order. The Bessel function has a branching point $y = y_\ell$.

The rule of selection of the appropriate branch of the solution for (4.1) and (3.4) follows from the analysis of a more general problem. The selection may be accomplished, for example, based on the following requirements: the solution of the problem for an inviscid fluid should be a limit of the solution of a 'viscous problem' when viscosity tends to zero. Another approach to problems of the kind consists in considering the evolution of an initial perturbation, in particular of the wave packet. In this case, the Fourier transform in (3.2) should be substituted by a Laplace transform, and the singular point in the equation is located in the complex plane rather than on the real axis. This automatically defines the rule of matching across this point and the selection of a solution branch.

These two approaches are equivalent, and give the rule first introduced into physics by Landau (1946) and into hydrodynamics by Lin (1955): a singular point located on the real axis should be matched in the complex plane y in the same manner as it would be matched in the case of a growing solution $\mathrm{Im}\,\omega > 0$ on the real axis. Using this rule one can readily obtain that at $k_x U' > 0$ a singular point is matched in the upper half-plane, and the wave with a negative phase velocity at $y < y_\ell$ corresponds to the exponentially damped solution at $y > y_\ell$:

$$(y - y_\ell)^{\frac{1}{4}} \exp\{-2[A(y - y_\ell)]^{\frac{1}{2}}\} \rightleftharpoons (y_\ell - y)^{\frac{1}{4}} \exp\{-2\mathrm{i}[A(y_\ell - y)]^{\frac{1}{2}}\}. \tag{4.3}$$

Note that branch II of the dispersion curve in figure 2(*c*) corresponds to the waves in the region (y_2, y_ℓ). For this branch the directions of the wave vector and group-velocity components along the y-axis are opposite. Thus the group velocity at $y > y_2$ is directed to the limiting point. The bounded internal-wave train asymptotically approaches the limiting point, with the wave-energy density increasing until dissipation or nonlinear effects appear.†

If the flow velocity U_m were relatively small, so that the limiting point were absent

† In flows with a vertical velocity gradient the critical layer separates the regions of propagation of the waves with different signs of energy density. Therefore at a finite Richardson number the waves can transit through the critical layer, in contrast with the limiting layer in a horizontally inhomogeneous flow.

in the presence of point y_2, a solution could be constructed using the radiation condition at $y > y_2$ for the wave transmitted through the barrier (y_1, y_2). The same procedure can be used in the presence of a limiting layer, since it allows for such a wave in the region (y_2, y_ℓ) only.

The problem of wave transmission through the barrier in the presence of a point of synchronism was analysed as applied to acoustic waves in parallel shear flows by Fabrikant (1976) and Gavrilenko & Zelekson (1977). A similar consideration is suitable for our case. Matching WKB solutions to the left of point y_2 to solution in the region $y > y_2$ is accomplished with the use of the Airy function (Bender & Orszag 1978). To match solutions in the regions $y < y_s$ and $y > y_s$, a standard equation is used for which the Whittaker functions are the solutions. Selection of appropriate branches of these functions is defined by Lin's rule. Subsequent crossing of point y_1 is similar to matching WKB solutions at point y_2. Omitting tedious computations (see Appendix), we write the reflection coefficient in its final form

$$R = \mathrm{i}\frac{1+\frac{1}{2}\pi\mu\{\mathrm{e}^{\mathrm{i}2\pi\mu-2\delta_1}+\mathrm{e}^{-2\delta_2}\}+\frac{1}{4}\mathrm{e}^{-2\delta-\mathrm{i}2\pi\mu}+O(\mu^2\mathrm{e}^{-2\delta})}{1-\frac{1}{2}\pi\mu\{\mathrm{e}^{\mathrm{i}2\pi\mu-2\delta_1}+\mathrm{e}^{-2\delta_2}\}-\frac{1}{4}\mathrm{e}^{-2\delta-\mathrm{i}2\pi\mu}+O(\mu^2\mathrm{e}^{-2\delta})}, \tag{4.4}$$

where

$$\delta_1 = \mathrm{i}\int_{y_1}^{y_s} n(y)\,\mathrm{d}y, \quad \delta_2 = \mathrm{i}\int_{y_s}^{y_2} n(y)\,\mathrm{d}y, \quad \delta = \delta_1+\delta_2, \quad \mu = -\frac{U''(y_s)}{2kU'(y_s)}. \tag{4.5}$$

Assumption of a smooth velocity profile gives $\delta_1, \delta_2, \delta \gg 1$; $|\mu| \ll 1$, then (4.4) yields

$$|R|^2 \simeq 1+\mathrm{e}^{-2\delta}+2\pi\mu\,\mathrm{e}^{-2\delta_1}. \tag{4.6}$$

It follows from (4.6) that the modulus of the reflection coefficient of the wave at the flow may be both larger and smaller than unity, i.e. the incident wave amplifies (overreflection) or damps depending on the ratio of the second and third terms and the sign of μ. If μ is not small, the third term makes the main contribution to (4.6), since $\delta_1 < \delta$. In particular, when the flow-velocity profile changes so that $y_2 \to \infty$, the second term vanishes. The third term is defined by the resonant wave-flow interaction at the point of synchronism. This mechanism is similar to that of wave generation by wind (Miles 1957). According to this, surface waves grow as a result of their interaction with the wind flow in the layer of coincidence. The sign of the third term in (4.6) is defined by the sign of μ, which depends on the velocity profile. In the case under consideration $k_x U' > 0$ the wave amplifies ($\mu > 0$) at $U''(y_s) < 0$ (with the energy transferred from the flow to the waves), and at $U''(y_s) > 0$ the inverse process takes place and the wave damps. The efficiency and character of the resonant interaction depend on the energy exchange between the wave and the particles of fluid with velocity close to that of the wave. Particles with velocities larger than the wave velocity slow down and give their energy to the wave, while particles with smaller velocities accelerate and withdraw energy from the wave. The difference between the number of 'fast' and 'slow' particles in the velocity intervals $U(y_s)+\mathrm{d}U$ and $U(y_s)-\mathrm{d}U$, where $\mathrm{d}U$ corresponds to particles efficiently interacting with the wave, defines the character of resonant interaction. One can show that this difference is proportional to μ. At $U''(y_s) = 0$ resonant wave-flow interaction is absent ($\mu = 0$) and the main role in (4.6) belongs to the second term. This term describes overreflection, which arises owing to the excitation in the region $y > y_2$ of the negative-energy wave and its contribution to the module of the reflection coefficient is always positive.

5. Waveguide modes in a jet-type flow

The possibility of internal-wave localization in flows with a jet-type velocity profile has been stated in §2.3. We consider this phenomenon in more detail. As follows from the analysis of the dispersion relations, localized waves moving against the flow ($k_x < 0$) with a phase speed $N/|k_x| - U_m < |c| < N/|k_x|$, and along the flow ($k_x > 0$) with $U_m - N/k_x < c < U_m$, are feasible in a parallel jet flow with the velocity maximum U_m. For definiteness, assume that $n^2(U_m) > 0$. The case of forward waves is of most interest, since localized waves propagating along the flow may grow owing to the mechanisms considered in §4. The potential hump $-K^2(y)$ for a jet flow at $U_m < (\omega+N)/k_x$ is given in figure 3(*b*). Assuming that the frequency ω is real, we determine the space spectrum and growth rate of the localized modes. Let us use the condition of mode formation

$$R_1 R_2 \exp\left\{2\mathrm{i}\int_{y_1}^{y_2} n(y)\,\mathrm{d}y\right\} = 1, \tag{5.1}$$

where R_1 and R_2 are the coefficients of reflection at the potential barriers (y_1, y_1') and (y_2, y_2'), which can be determined from formulae similar to (4.4). To find $\kappa = \mathrm{Re}\, k_x$ we transform (5.1) to

$$\pi(l+\tfrac{1}{2}) = \int_{y_1}^{y_2} \left\{k_z^2 \frac{[\omega-\kappa U(y)]^2}{N^2-[\omega-\kappa U(y)]^2} - \kappa^2\right\}^{\frac{1}{2}} \mathrm{d}y, \tag{5.2}$$

where l is the mode number, and for the increment $\gamma = \mathrm{Im}\, k_x$

$$\gamma = -\tfrac{1}{4}[\mathrm{e}^{-2\delta_1} + \mathrm{e}^{-2\delta_2} + 2\pi(\mu_1 \mathrm{e}^{-2\delta_1'} + \mu_2 \mathrm{e}^{-2\delta_2'})] \times \left\{\int_{y_1}^{y_2} \left[\kappa + \frac{k_z^2(\omega-\kappa U)\,UN^2}{[N^2-(\omega-\kappa U)^2]^2}\right]\left[k_z^2 \frac{(\omega-\kappa U)^2}{N^2-(\omega-\kappa U)^2} - \kappa^2\right]^{-\frac{1}{2}} \mathrm{d}y\right\}^{-1}, \tag{5.3}$$

where

$$\delta_{1,2} = \mathrm{i}\int_{y_{1,2}}^{y_{1,2}'} n(y)\,\mathrm{d}y, \quad \delta_{1,2}' = \mathrm{i}\int_{y_{1,2}}^{y_{s1,2}} n(y)\,\mathrm{d}y, \quad \mu_{1,2} = -\frac{U''(y_{s1,2})}{2\kappa U'(y_{s1,2})}. \tag{5.4}$$

The points corresponding to the integration limits in (5.4) are given in figure 3(*b*). It can be easily shown that at $|R_1 R_2| > 1$ the increment of the localized internal wave is positive $\gamma > 0$. To estimate the increments, consider a flow with the Gaussian velocity profile

$$U(y) = U_m \exp\{-y^2/L^2\}. \tag{5.5}$$

The dimensionless space increment $\tilde{\gamma} = \gamma L$ as a function of the dimensionless wave number $\tilde{k} = kL$ is given in figure 4 for $k_z L = 1$, $NL/U_m = 1$. The broken lines describe the families of modes with different Mach numbers $\tilde{c} = c/U_m$, where $c = \omega/\kappa$. The points on these lines correspond to a discrete mode spectrum for each c. In the vicinity of the point

$$k_0 = \frac{N}{U_m - c}$$

the spectrum becomes more and more dense. The localized modes in a jet of the type (5.5) increase if $\tilde{c} > \tilde{c}_0 = 0.53$. At smaller velocities $\gamma < 0$. The second derivative of the function (5.5) at the points of synchronism changes the sign at $\tilde{c}_1 = 0.61$. Proximity of the values of $\tilde{c}_0$ and $\tilde{c}_1$ is indicative of a greater effect of the wave–flow resonance on the growth rate as compared with the negative-energy wave radiation mechanism.

At $\kappa > k_0$ the above picture changes qualitatively. In particular, on the potential

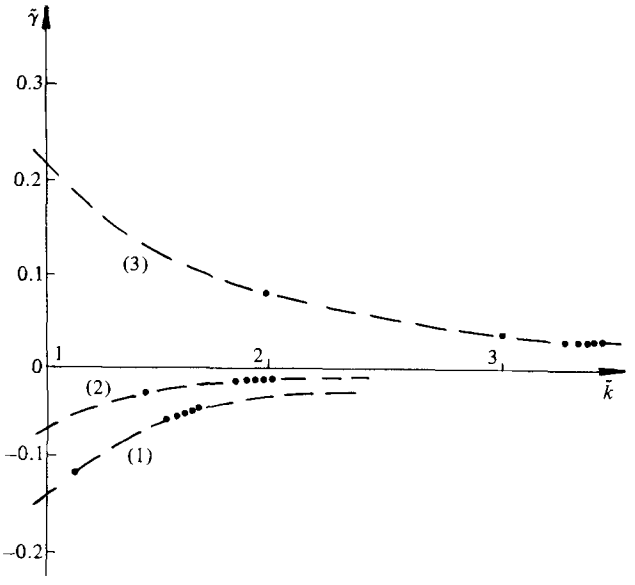

FIGURE 4. Dimensionless space increment as a function of dimensionless wave number for internal waves at $k_z L = 5$, $NL/U_m = 1$: (1) $c = 0.3U_m$; (2) $c = 0.5U_m$; (3) $c = 0.7U_m$.

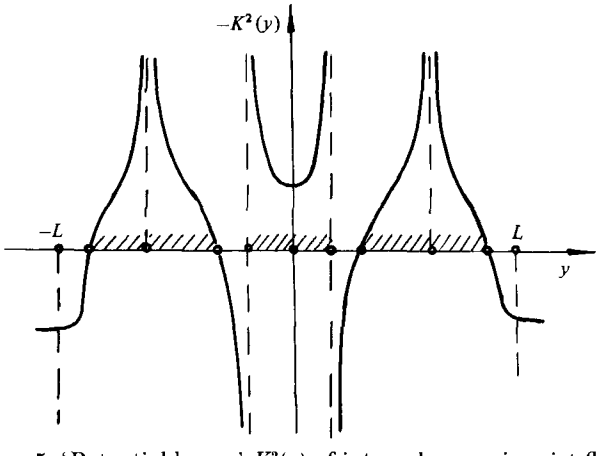

FIGURE 5. 'Potential hump'-$K^2(y)$ of internal waves in a jet flow in the presence of limiting layers.

hump at $\kappa = k_0$ two limiting layers appear in the vicinity of the jet centre and the region between them is non-transparent for the waves with the given parameters (figure 5). As κ increases, the limiting layers move from the centre of the jet to the periphery. In this situation no mode forms.

6. Conclusion

The consideration given above shows that horizontally inhomogeneous flows may essentially affect internal-wave propagation. In particular, the effects of wave trapping by limiting layers and amplification by the modes in a jet may result in an

increase in the internal-wave field in the region of the intense flow. It is not excluded that the excess of the internal-wave amplitude in the synoptic vortex over the background level observed by Dykman & Kiselyova (1981), is also governed by these mechanisms. The wave-vector orientation of the internal-wave packets perpendicular to the flow when approaching the limiting point may be one of the causes of significant anisotropy of the internal-wave spectra in the flow region observed by Frankingnoul (1974).

Upon the whole, however, it should be pointed out that the model considered here is quite simplified, since it does not take into account a lot of factors, in particular, the Earth's rotation, a complex three-dimensional structure of real fields of the flow velocity and stratification, as well as their non-stationary character. Further development of the theory requires consideration of all the mentioned factors, which essentially complicates the investigation. At the same time, our analysis carried out for a simple model made it possible to study effects of the kind that may be essential in more complex situations.

The authors are grateful to Professor L. A. Ostrovsky and Professor V. I. Talanov for fruitful discussions.

Appendix

To obtain an expression for the coefficient of wave reflection at the flow with a monotonic velocity profile (figure 3(*a*)), we match WKB solutions of (3.4) and (3.5) throughout the region of the variable y. As shown in §4, only the wave with a group velocity oriented from point y_2 may exist in the region (y_2, y_ℓ). Using this as the radiation condition at $y > y_2$, it is sufficient to determine the coefficient of reflection at the potential barrier (y_1, y_2). Formal consideration of solutions for (3.4) and (3.5) requires introduction of a large parameter. We introduce a new variable $\tilde{y} = y/L$ and write (3.4) and (3.5) in the dimensionless form

$$\left.\begin{aligned} &\xi'' + K^2(\tilde{y})\,\xi = 0, \\ &K^2(\tilde{y}) = \alpha_0^2\,\tilde{n}^2 + \frac{\Omega''}{\Omega} - 2\left(\frac{\Omega'}{\Omega}\right)^2, \\ &\tilde{n}^2 = \frac{k_z^2}{k^2}\frac{\Omega^2}{N^2-\Omega^2} - q^2, \\ &\alpha_0^2 = k^2L^2, \quad q^2 = \frac{k_x^2}{k^2}, \end{aligned}\right\} \tag{A 1}$$

where k is the wavenumber at $U = 0$. For the sake of simplicity, the tildes over y and n are omitted below.

The asymptotic form of the general solution (A 1) in the region $y > y_2$ is

$$\xi = A_{\mathrm{I}}(y_2, y) + B_{\mathrm{I}}(y, y_2). \tag{A 2}$$

We use the notation for WKB solutions adopted by Heading (1962*b*):

$$(y_i, y) \equiv n^{-\frac{1}{2}} \exp\left\{\mathrm{i}\alpha_0 \int_{y_i}^{y} n(y)\,\mathrm{d}y\right\}, \tag{A 3}$$

$$(y, y_i) \equiv n^{-\frac{1}{2}} \exp\left\{-\mathrm{i}\alpha_0 \int_{y_i}^{y} n(y)\,\mathrm{d}y\right\}. \tag{A 4}$$

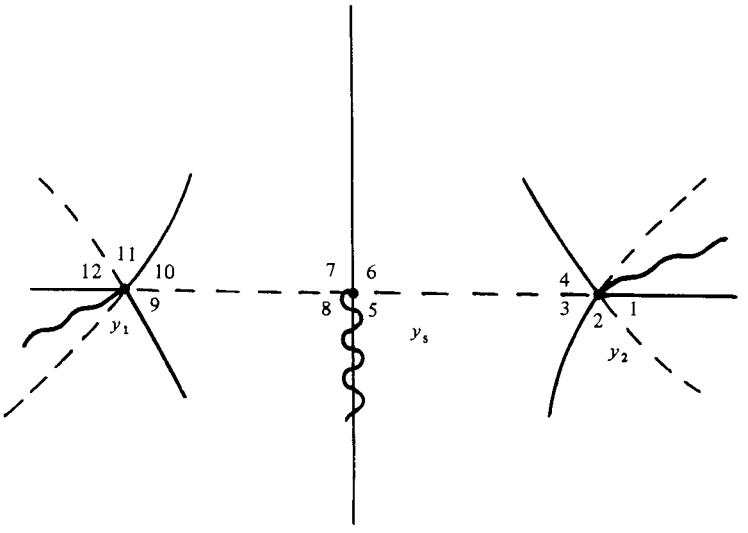

FIGURE 6. Complex y-plane with the turning points $y_{1,2}$ and the point of synchronism y_s: – – –, Stokes lines; ——, antiStokes lines; ~~, branch cuts.

For WKB solutions in a complex plane, solutions increasing or decreasing over α_0 have indices d and s respectively. In the intermediate case the index is omitted.

Figure 6 shows a complex plane of variable y with the Stokes and antiStokes lines, and the branch cuts defining an unambiguous choice of the branch of solution. It is known that the Stokes phenomenon consists in a stepwise variation of the asymptotic presentation of the solution when certain lines on the complex plane, so-called Stokes lines, are crossed (Heading 1962*b*). On these lines, the arguments in the exponents in (A 3) and (A 4) are real:

$$\mathrm{Im}\left\{\mathrm{i}\alpha_0 \int_{y_i}^{y} n(y)\,\mathrm{d}y\right\} = 0.$$

Therefore one of the WKB solutions on the Stokes lines grows exponentially with α_0, and the other one decreases. When crossing the Stokes line, the coefficient in (A 2) changes abruptly at the WKB solution (A 3) or (A 4), decreasing on this line. The value of the jump is equal to the product of the coefficient at the growing solution and a certain constant (the so-called Stokes constant) which corresponds to the given Stokes line. The Stokes constants are defined by standard equations.

The Stokes lines for (A 1) are given in figure 6 (broken lines). Beyond the Stokes lines, arguments in the exponents of solutions (A 3) and (A 4) are complex. There are lines (antiStokes lines) on which the given above arguments are imaginary:

$$\mathrm{Re}\left\{\mathrm{i}\alpha_0 \int_{y_i}^{y} n(y)\,\mathrm{d}y\right\} = 0.$$

Solutions (A 3) and (A 4) on the antiStokes lines oscillate as α_0 varies. When these lines are crossed, the signs of the real parts of the arguments in the WKB solutions (A 3) and (A 4) and correspondingly their behaviour as functions of α_0 change. This results in the change of the indices d and s of these functions. The antiStokes lines are shown in figure 6 by heavy curves. The wavy curves show the branch cuts. These

are drawn from points y_1 and y_2 and define the unambiguous choice of the branch of function $n(y)$ in the region (y_1, y_2),

$$n(y) = |n|\,\mathrm{e}^{-\frac{1}{2}\mathrm{i}\pi},$$

and correspondingly of the function $n^{-\frac{1}{2}}$. The branch cut drawn from the point of synchronism y_s is defined by the rule of matching (see §4).

The Stokes-like pattern is constructed based on standard equations. In the vicinity of the turning points the construction is carried out conventionally using the Airy equation. In the vicinity of the point of synchronism the standard equation was obtained by Gavrilenko & Zelekson (1978) according to Fok (1931):

$$\frac{\mathrm{d}^2\xi}{\mathrm{d}y^2} + \left[\alpha_0^2 n^2 + 2s_0'^2\left(\mathrm{i}\frac{\mu}{s_0} - \frac{1}{s_0^2}\right)\right]\xi = 0, \tag{A 5}$$

where

$$\mu = -\frac{U''}{2\alpha_0 q U'(y_s)}, \quad s_0 = \alpha_0 \int_{y_s}^{y} n(y)\,\mathrm{d}y. \tag{A 6}$$

Equation (A 5) has the same singularity as (A 1) and coincides with (A 1) far from y_s. The exact solution of (A 5) is

$$\xi = \frac{1}{s_0'^{\frac{1}{2}}}\{C_1 W_{\mu,\frac{1}{2}}(2\mathrm{i}s_0) + C_2 W_{-\mu,\frac{1}{2}}(-2\mathrm{i}s_0)\}, \tag{A 7}$$

where $s_0' = \alpha_0 n(y)$, C_1 and C_2 are arbitrary constants, and $W_{\mu,\frac{1}{2}}$ and $W_{-\mu,\frac{1}{2}}$ are the Whittaker functions. Since the parameter α_0 is large, $|s_0|$ is large even at small $|y-y_s|$. Instead of the Whittaker functions one can use their asymptotic expansion for larger values $|s|$ of the variable $s = 2is_0$ (note that $\arg s$ coincides with $\arg(y-y_s)$). Then the asymptotic expansions are at the same time representations of the solution of (A 1). At $|s| \gg 1$, instead of (A 7) one can write

$$\left.\begin{aligned} \xi &= \alpha Q + \beta P = n^{-\frac{1}{2}}(\alpha\tilde{Q} + \beta\tilde{P}), \\ \tilde{P} &= \mathrm{e}^{-\frac{1}{2}s}\, s^{\mu}, \quad \tilde{Q} = \mathrm{e}^{\frac{1}{2}s}\, s^{-\mu}. \end{aligned}\right\} \tag{A 8}$$

Here α and β are arbitrary constants. The Stokes phenomenon for (A 8) was studied by Heading (1962*a*), who obtained the Stokes lines $\arg s = \pi n$, the antiStokes lines $\arg s = \pi(\frac{1}{2}+n)$ and the Stokes constants

$$T_n = 2\pi\mathrm{i}\,\mathrm{e}^{-4\pi\mathrm{i}n\nu\mu}/\Gamma(2+\nu\mu)\,\Gamma(-1+\nu\mu), \tag{A 9}$$

$$\nu = (-1)^n, \quad n = 0, \pm 1, \pm 2, \ldots,$$

where Γ is the gamma function. The lines in figure 6 are drawn according to Heading (1962*a*).

Let us construct an asymptotic representation of the solution of (A 1). If the coefficients A_{I} and B_{I} in (A 2) at $y > y_2$ are known, we must find the coefficients A_{II} and B_{II} at $y < y_1$ in the expression

$$\xi = A_{\mathrm{II}}(y_1, y) + B_{\mathrm{II}}(y, y_1).$$

Consider points y_2, y_s and y_1. Let us construct asymptotic representations successively in regions 1, 2 and so on (figure 6) according to the procedure described by Heading (1962*b*).

Matching across point y_2

1: $A_{\mathrm{I}}(y_2, y)_{\mathrm{d}} + B_{\mathrm{I}}(y, y_2)_{\mathrm{s}}$;

2: $A_{\mathrm{I}}(y_2, y)_{\mathrm{d}} + (B_{\mathrm{I}} - \mathrm{i}A_{\mathrm{I}})(y, y_2)_{\mathrm{s}}$;

in crossing the Stokes line from region 1 to region 2, the coefficient changes abruptly at the decreasing solution, the Stokes constant is $-\mathrm{i}$.

3: $A_{\mathrm{I}}(y_2, y)_{\mathrm{s}} + (B_{\mathrm{I}} - \mathrm{i}A_{\mathrm{I}})(y, y_2)_{\mathrm{d}}$;

the interchange of indices corresponds to the change in behaviour of the functions (A 3) and (A 4).

3–4: the region of the real axis $y < y_2$ is the Stokes line.

The WKB method does not allow for determination of the coefficient at the decreasing solution in this line. However, for (A 1) there is an invariant (Heading 1962*b*)

$$\mathrm{Im}\,(\xi'\xi^*) = \mathrm{const.} \tag{A 10}$$

Use of this invariant makes it possible to determine the Stokes constant in the Stokes line. When crossed, this line is equal to half of the Stokes constant, i.e. in our case it is $-\frac{1}{2}\mathrm{i}$. Then

$$A_{3,4}(y_2, y)_{\mathrm{s}} + B_{3,4}(y, y_2)_{\mathrm{d}} = [A_{\mathrm{I}} - \tfrac{1}{2}\mathrm{i}(B_{\mathrm{I}} - \mathrm{i}A_{\mathrm{I}})]\ (y_2, y)_{\mathrm{s}} + (B_{\mathrm{I}} - \mathrm{i}A_{\mathrm{I}})(y, y_2)_{\mathrm{d}}.$$

Finally we obtain a relation in the matrix form

$$\begin{pmatrix} A_{3,4} \\ B_{3,4} \end{pmatrix} = \begin{pmatrix} \frac{1}{2} & -\frac{1}{2}\mathrm{i} \\ -\mathrm{i} & 1 \end{pmatrix} \begin{pmatrix} A_{\mathrm{I}} \\ B_{\mathrm{I}} \end{pmatrix}. \tag{A 11}$$

Transition from point y_2 to point y_{s}

When we pass over from the basic functions $(y_2, y)_{\mathrm{s}}$ and $(y, y_2)_{\mathrm{d}}$ to the functions $(y_{\mathrm{s}}, y)_{\mathrm{d}}$ and $(y, y_{\mathrm{s}})_{\mathrm{s}}$ the coefficients transform as follows

$$\begin{pmatrix} A_{5,6} \\ B_{5,6} \end{pmatrix} = \begin{pmatrix} \mathrm{e}^{-\delta_2} & 0 \\ 0 & \mathrm{e}^{\delta_2} \end{pmatrix} \begin{pmatrix} A_{3,4} \\ B_{3,4} \end{pmatrix}, \tag{A 12}$$

where

$$\delta_2 = \mathrm{i}\alpha_0 \int_{y_{\mathrm{s}}}^{y_2} n(y)\,\mathrm{d}y.$$

Matching across point y_{s}

Consider (A 8) on the real axis at $y > y_{\mathrm{s}}$:

$$\left.\begin{aligned} Q_{\mathrm{d}} &= n^{-\frac{1}{2}}\mathrm{e}^{\frac{1}{2}s - \mu \ln s} \approx n^{-\frac{1}{2}}\mathrm{e}^{\frac{1}{2}s} = (y_{\mathrm{s}}, y)_{\mathrm{d}}, \\ P_{\mathrm{s}} &= n^{-\frac{1}{2}}\mathrm{e}^{-\frac{1}{2}s + \mu \ln s} \approx n^{-\frac{1}{2}}\mathrm{e}^{-\frac{1}{2}s} = (y, y_{\mathrm{s}})_{\mathrm{s}}. \end{aligned}\right\} \tag{A 13}$$

It follows from (A 13) that

$$\alpha_+ = A_{5,6}, \quad \beta_+ = B_{5,6},$$

where α_+ and β_+ are the values of α and β at $y > y_{\mathrm{s}}$. On the real axis at $y < y_{\mathrm{s}}$ the functions Q and P behave as follows:

$$\begin{aligned} Q &= n^{-\frac{1}{2}}\mathrm{e}^{\frac{1}{2}s - \mathrm{i}\pi\mu - \mu \ln |s|} \simeq n^{-\frac{1}{2}}\mathrm{e}^{\frac{1}{2}s - \mathrm{i}\pi\mu} = \mathrm{e}^{-\mathrm{i}\pi\mu}\,(y_{\mathrm{s}}, y)_{\mathrm{s}}, \\ P &= n^{-\frac{1}{2}}\mathrm{e}^{-\frac{1}{2}s + \mathrm{i}\pi\mu + \mu \ln |s|} \simeq n^{-\frac{1}{2}}\mathrm{e}^{-\frac{1}{2}s + \mathrm{i}\pi\mu} = \mathrm{e}^{\mathrm{i}\pi\mu}\,(y, y_{\mathrm{s}})_{\mathrm{d}}, \end{aligned} \tag{A 14}$$

where $s = |s|\,e^{i\pi}$. The real axis is the Stokes line, the same as for matching across point y_2. Here Stokes constant on the line is also half of that when the line is crossed. To sum up, the relation between $A_{5,6}$, $B_{5,6}$ and $A_{7,8}$, $B_{7,8}$ is

$$\begin{aligned}
5\text{–}6:&\quad \alpha_+ Q_d + \beta_+ P_s = A_{5,6}(y_s, y)_d + B_{5,6}(y, y_s)_s;\\
6:&\quad \alpha_+ Q_d + [\beta_+ + \tfrac{1}{2}T_0\alpha_+]P_s;\\
7:&\quad \alpha_+ Q_s + [\beta_+ + \tfrac{1}{2}T_0\alpha_+]P_d;\\
7\text{–}8:&\quad \{\alpha_+ + \tfrac{1}{2}T_1[\beta_+ + \tfrac{1}{2}T_0\alpha_+]\}Q_s + [\beta_+ + \tfrac{1}{2}T_0\alpha_+]P_d\\
&\qquad = \alpha_- Q_s + \beta_- P_d = \alpha_- e^{-i\pi\mu}(y_s, y)_s + \beta_- e^{i\pi\mu}(y, y_s)_d\\
&\qquad = A_{7,8}(y_s, y)_s + B_{7,8}(y, y_s)_d.
\end{aligned}$$

Here α_- and β_- are the coefficients in (A 8) in the region $y < y_s$, and T_0 and T_1 are the Stokes constants obtaned from (A 9):

$$T_0 = \frac{2\pi i}{\Gamma(2+\mu)\,\Gamma(-1+\mu)},$$

$$T_1 = \frac{2\pi i}{\Gamma(2-\mu)\,\Gamma(-1-\mu)}.$$

As a result we have

$$\begin{pmatrix} A_{7,8} \\ B_{7,8} \end{pmatrix} = \begin{pmatrix} e^{-i\pi\mu} - e^{3i\pi\mu}\gamma(\mu)\gamma(-\mu) & i\,e^{3\pi i\mu}\gamma(\mu) \\ i\,e^{i\pi\mu}\gamma(-\mu) & e^{i\pi\mu} \end{pmatrix} \begin{pmatrix} A_{5,6} \\ B_{5,6} \end{pmatrix}, \tag{A 15}$$

where

$$\gamma(\mu) = \frac{\pi}{\Gamma(2-\mu)\,\Gamma(-1-\mu)}.$$

The other transition matrices are found in a similar way.

Transition from point y_s to point y_1

$$\begin{pmatrix} A_{9,10} \\ B_{9,10} \end{pmatrix} = \begin{pmatrix} e^{-\delta_1} & 0 \\ 0 & e^{\delta_1} \end{pmatrix} \begin{pmatrix} A_{7,8} \\ B_{7,8} \end{pmatrix}, \tag{A 16}$$

where

$$\delta_1 = i\alpha_0 \int_{y_1}^{y_s} n(y)\,dy.$$

Matching across point y_1

$$\begin{pmatrix} A_{II} \\ B_{II} \end{pmatrix} = \begin{pmatrix} \frac{1}{2} & i \\ \frac{1}{2}i & 1 \end{pmatrix} \begin{pmatrix} A_{9,10} \\ B_{9,10} \end{pmatrix}. \tag{A 17}$$

Combining (A 11), (A 12) and (A 15)–(A 17), we obtain

$$\begin{pmatrix} A_{II} \\ B_{II} \end{pmatrix} = \begin{pmatrix} \frac{1}{2} & i \\ \frac{1}{2}i & 1 \end{pmatrix} \begin{pmatrix} e^{-\delta_1} & 0 \\ 0 & e^{\delta_1} \end{pmatrix} \begin{pmatrix} e^{-i\pi\mu} e^{3\pi i\mu}\gamma(\mu)\gamma(-\mu) & i\gamma(\mu)e^{3\pi i\mu} \\ i\,e^{i\pi\mu}\gamma(-\mu) & e^{i\pi\mu} \end{pmatrix}$$
$$\times \begin{pmatrix} e^{-\delta_2} & 0 \\ 0 & e^{\delta_2} \end{pmatrix} \begin{pmatrix} \frac{1}{2} & -\frac{1}{2}i \\ -i & 1 \end{pmatrix} \begin{pmatrix} A_I \\ B_I \end{pmatrix}. \tag{A 18}$$

Relation (A 18) and the radiation condition $B_{II} = 0$ (see (A 3)) allow us to obtain reflection and transmission coefficients of the wave incident to the barrier (see §4). Then, taking into account that $\mu \ll 1$, we have (4.4).

REFERENCES

ACHESON, D. J. 1976 On over-reflection. *J. Fluid Mech.* **77**, 433–472.

AHMED, B. M. & ELTAYEB, I. A. 1980 On the propagation, reflection, transmission and stability of atmospheric Rossby–gravity waves on a beta-plane in the presence of latitudinally sheared zonal flows. *Proc. R. Soc. Lond.* A **298**, 45–85.

BARCILON, A. & DRAZIN, P. G. 1972 Dust devil formation. *Geophys. Fluid Dyn.* **4**, 147–158.

BASOVICH, A. YA. & TALANOV, V. I. 1977 Transformation of short surface waves on an inhomogeneous flow. *Izv. Akad. Nauk SSSR, Fiz. Atmos. i Okeana* **13**, 766–773.

BENDER, C. M. & ORSZAG, S. A. 1978 *Advanced Mathematical Methods for Scientists and Engineers.* McGraw-Hill.

BOOKER, J. R. & BRETHERTON, F. P. 1967 The critical layer for internal gravity waves in a shear flow. *J. Fluid Mech.* **27**, 513–539.

DYKMAN, V. Z. & KISELYOVA, O. A. 1981 Relation between fine structure, internal waves and small-scale turbulence. *Okeanologiya* **21**, 605–612.

FABRIKANT, A. L. 1976 Acoustic wave-parallel flow resonant interaction. *Akust. Zh.* **22**, 107–114.

FOK, V. A. 1931 Approximate representation of the wave functions of penetrating orbits. *Dokl. Akad. Nauk SSSR* **1**, 241–244.

FRANKIGNOUL, C. J. 1974 Observed anisotropy of spectral characteristics of internal waves induced by low-frequency currents. *J. Phys. Oceanogr.* **4**, 625–634.

FRITTS, D. C. 1978 The nonlinear gravity wave – critical level interaction. *J. Atmos. Sci.* **35**, 397–413.

GARGETT, A. E. & HUGHES, R. A. 1972 On the interactions of surface and internal waves. *J. Fluid Mech.* **52**, 179–191.

GAVRILENKO, V. G. & ZELEKSON, L. A. 1977 Sound amplification in an inhomogeneous flow. *Akoust. Zh.* **23**, 867–872.

HEADING, J. 1962*a* The Stokes phenomenon and the Whittaker function. *J. Lond. Math. Soc.* **37**, 195–208.

HEADING, J. 1962*b* *An Introduction to Phase-Integral Methods.* Wiley.

LANDAU, L. 1946 On the vibrations of the electronic plasma. *J. Phys. USSR* **10**, 25.

LIN, C. C. 1955 *The Theory of Hydrodynamic Stability.* Cambridge University Press.

MILES, J. W. 1957 On the generation of surface waves by wind. *J. Fluid Mech.* **3**, 185–204.

MODE GROUP 1978 The Mid-Ocean Dynamics Experiment. *Deep-Sea Res.* **25**, 859–910.

OLBERS, D. J. 1981 The propagation of internal waves in a geostrophic current. *J. Phys. Oceanogr.* **11**, 1224–1233.

PHILLIPS, O. M. 1973 On the interaction between internal and surface waves. *Phys. Atmos. Ocean* **9**, 954–961.

PHILLIPS, O. M. 1977 *The Dynamics of the Upper Ocean*, 2nd edn. Cambridge University Press.

RUDDICK, B. R. & JOYCE, T. M. 1979 Observation of the interaction between the internal wave field and low-frequency flows in the North Atlantic. *J. Phys. Oceanogr.* **9**, 498–517.

SMITH, R. 1975 The reflection of short gravity waves on a nonuniform current. *Math. Proc. Camb. Phil. Soc.* **78**, 517–525.

THORPE, S. A. 1981 An experimental study of critical layers. *J. Fluid Mech.* **103**, 321–344.

WHITHAM, G. B. 1974 *Linear and Nonlinear Waves.* Wiley.